

Title: The VvNIP2;1 aquaporin is a grapevine silicon channel

Authors: Henrique Noronha^{1,2*}, Angélica Silva¹, Namiki Mitani-Ueno³, Carlos Conde^{4,5}, Farzana Sabir^{6,7}, Catarina Prista⁷, Graça Soveral⁶, Paul Isenring⁸, Jian Feng Ma³, Richard R Bélanger⁹, Hernâni Gerós^{1,2,10}

Affiliations:

¹ Centre of Molecular and Environmental Biology (CBMA), Department of Biology, University of Minho, Braga, Portugal.

² Centre for the Research and Technology of Agro-Environmental and Biological Sciences (CITAB), University of Trás-os-Montes e Alto Douro, Vila Real, Portugal.

³ Institute of Plant Science and Resources, Okayama University, Chuo 2-20-1, Kurashiki 710-0046, Japan

⁴ i3S, Instituto de Investigação e Inovação em Saúde, Universidade do Porto

⁵ IBMC, Instituto de Biologia Molecular e Celular, Universidade do Porto

⁶ Research Institute for Medicines (iMed.Ulisboa), Faculty of Pharmacy, Universidade de Lisboa, Lisboa, Portugal.

⁷ LEAF, Linking Landscape, Environment, Agriculture and Food, and DRAT, Dept. de Recursos Biológicos, Ambiente e Território, Instituto Superior de Agronomia, Universidade de Lisboa, Tapada da Ajuda, 1349-017 Lisboa

⁸ Nephrology Group, L'Hôtel-Dieu de Québec Institution, Department of Medicine, Faculty of Medicine, Université Laval, Québec, Québec G1R 2J6, Canada

⁹ Département de Phytologie, Faculté des Sciences de l'Agriculture et de l'Alimentation (FSAA), Université Laval, Québec, Québec G1V 0A6, Canada

¹⁰ Centre of Biological Engineering (CEB), Department of Engineering, University of Minho, Braga, Portugal.

*Corresponding author

E-mail: henriquenoronha@bio.uminho.pt
orcid.org/0000-0002-4809-6609

Authors e-mails:

HN: henriquenoronha@bio.uminho.pt

AS: angelicasilva@bio.uminho.pt

NM: namiki-m@rib.okayama-u.ac.jp

CC: cconde@ibmc.up.pt

FS: fsabir@isa.ulisboa.pt

CP: cprista@isa.ulisboa.pt

GS: gsoveral@ff.ulisboa.pt

PI: Paul.Isenring@crchudequebec.ulaval.ca

RB: Richard.Belanger@fsaa.ulaval.ca

JM: maj@rib.okayama-u.ac.jp

HG: geros@bio.uminho.pt

Highlight: The grapevine (*Vitis vinifera*) aquaporin VvNIP2;1 is a silicon channel localized at the plasma membrane highly expressed in roots.

Abstract

Silicon (Si) supplementation has been shown to improve plant tolerance to different stresses and its accumulation in the aerial organs is mediated by NIP2;1 aquaporins (Lsi channels) and Lsi2-type exporters in roots. In the present study, we tested the hypothesis that grapevine expresses a functional NIP2;1 that accounts for root Si uptake and, eventually, Si accumulation in leaves. Own-rooted grapevine cuttings of the cultivar Vinhão accumulated over 0.2 % Si (dw) in leaves when irrigated with 1.5 mM Si for one month, while Si was undetected in control leaves. Real-time PCR showed that *VvNIP2;1* was highly expressed in roots and in green berries. The transient transformation of tobacco leaf epidermal cells mediated by *Agrobacterium tumefaciens* confirmed VvNIP2;1 localization at the plasma membrane. Transport experiments in oocytes showed that VvNIP2;1 mediates Si and arsenite uptake, whereas permeability studies revealed that VvNIP2;1 expressed in yeast is unable to transport water and glycerol. Si supplementation to pigmented grape cultured cells (cv. Gamay Freáux) had no impact on the total phenolic and anthocyanin content, as well as the growth rate and *VvNIP2;1* expression. Long-term experiments should help determine the extent of Si uptake over time and if grapevine can benefit from Si fertilization.

Key-words:

Aquaporin; cv. Vinhão; Grapevine; Nodulin-26 like Intrinsic Protein; Silicon transport; *Vitis vinifera*; VvNIP2;1; Water transport.

Introduction

Silicon (Si) is the most abundant mineral element in the earth crust, and the benefits of its supplementation for plants have been established in response to a plethora of biotic and abiotic stresses (Ma, 2004; Coskun *et al.*, 2019). In spite of this, Si transport mechanism remained elusive for long time until the identification and characterization of the first Si channels and transporters. Plant species have been classified according to their shoot Si concentration as active (> 1.5 % dw), passive (0.5-1.5 % dw) and rejective (< 0.5 % dw) accumulators. However, new molecular tools suggest a dichotomous partition whereby plants have the ability or not to accumulate Si (Ma and Takahashi, 2002; Hodson *et al.*, 2005; Mitani and Ma, 2005; Coskun *et al.*, 2019). Studies using rice mutants with low Si concentration led to the identification and characterization of the first plant Si channel, Lsi1 (Low silicon rice 1; Ma *et al.*, 2006). Since then, similar channels have been identified and characterized in monocots like barley (*Hordeum vulgare*; Chiba *et al.*, 2009; Yamaji *et al.*, 2012), wheat (*Triticum aestivum*; Montpetit *et al.*, 2012) and maize (*Zea mays*; Mitani *et al.*, 2009), in dicots including pumpkin (*Cucurbita moschata*; Mitani *et al.*, 2011) and soybean (*Glycine max*; Deshmukh *et al.*, 2013), cucumber (*Cucumis sativus*; Sun *et al.*, 2017), tomato (*Solanum lycopersicum*; Sun *et al.*, 2020) and in the primitive vascular plant *Equisetum arvense* (Grégoire *et al.*, 2012).

The channel-type Lsi1 and its homologs are NIP2 aquaporins (Nodulin-26 like Intrinsic Protein) that belong to the MIP (Membrane Intrinsic Protein) superfamily (Noronha *et al.*, 2016). NIPs have been shown to transport a variety of substrates including water (Mitani-Ueno *et al.*, 2011), hydrogen peroxide (Katsuhara *et al.*, 2014), glycerol (Cabello-Hurtado and Ramos 2004), metalloids (Ma *et al.*, 2008; Bienert *et al.*, 2008; Zhao *et al.*, -2010) and urea (Wallace and Roberts, 2005). More recently, NIP3s Si channels were identified in *Equisetum arvense* (Grégoire *et al.*, 2012). Lsi2-type transporters have also been described, which contrarily to Lsi1, are active exporters energized by the plasma membrane proton gradient (Ma *et al.*, 2007). Both Lsi1s and Lsi2 are important for high Si accumulation in plants (Sun *et al.*, 2020).

The first molecular and functional characterization of grapevine NIPs (NIP1;1, NIP5;1, and NIP6;1) occurred very recently (Sabir *et al.*, 2020). Their ability to transport water and glycerol was studied, and yeast growth assays suggest that some facilitate the transmembrane flux of metalloids (As, B, and Se) and the heavy metal Cd. In the present study, we aimed to test the hypothesis that grapevine expresses a

functional NIP2;1 that could account for root Si uptake and, eventually, Si accumulation in leaves. The accumulation of Si in leaves was tested in own-rooted grapevine cuttings of the cultivar Vinhão when irrigated with a 1.5 mM Si solution for one month. Real-time PCR studies were performed in samples from field-grown plants and rooted cuttings of the same cultivar and in pigmented cultured cells (cv. Gamay Freáux) to evaluate tissue-specific and regulation of *VvNIP2;1* expression. *VvNIP2;1* was cloned and its subcellular localization assessed through *Agrobacterium*-mediated transformation of *Nicotiana tabacum* epidermal cells. *VvNIP2;1* was functionally characterized in yeast cells by stopped-flow fluorescence and drop test growth assays. Conclusive results regarding the capacity of *VvNIP2;1* to transport Si and arsenite were obtained after expression studies in oocytes.

Material and Methods

In silico studies

Protein sequences were obtained from the database of the National Center of Biotechnology (NCBI). Protein alignment was performed by Prankster and the result was visualized in Genedoc (Nicholas *et al.*, 1997). Phylogenetic trees were constructed using the Maximum Likelihood method in Mega7 (Kumar *et al.*, 2016). The sequences accession numbers used were: *VvNIP1;5*, GSVIVT01021274001; *VvNIP3;1*, GSVIVT01034224001; *VvNIP3;2*, GSVIVT01019729001; *VvNIP2;1*, GSVIVT01011407001; *OsNIP2;1*, Q6Z2T3; *ZmNIP2;1*, Q19KC1; *GmNIP2;1*, C6TKR9; *PtNIP2;1*, B9IJY1; *SINIP2;1*, K4BEQ5; *OsNIP1;1*, Q40746; *OsNIP1;3*, Q0DK16; *OsNIP2;2*, Q67WJ8; *OsNIP3;1*, Q0IWF3; *SINIP1;1*, A0A3Q7F357; *SINIP1;3*, A0A3Q7FYL3; *SINIP3;1*, A0A3Q7FT05; *PtNIP1;1*, B9H2D3; *PtNIP1;2*, B9I1G4; *PtNIP3;1*, B9GVJ4; *PtNIP3;2*, B9GMB9; *ZmNIP1;1*, A0A1D6M054; *ZmNIP1;2*, K7VHT0; *Lsi2*, Q10SY9; *VvLsi2*, GSVIVT01028896001; *HvLsi2*, C6KYS0; *ZmLsi2*, C7G3B4.

The grapevine M1, M4 and 101.14 rootstock NIP2;1 sequences were obtained from the website www.genomes.cribi.unipd.it/grape/serres/ (Corso *et al.*, 2015). The NIP2;1 sequence for the 1103P rootstock was obtained using RNAseq raw data deposited at NCBI/sra (PRJNA342391; Cochetel *et al.*, 2017), which was analyzed at Kbase (Arkin *et al.*, 2018). HISAT2 and Cufflinks were used to map and assemble transcripts that were visualized with IGV (James *et al.*, 2011) to retrieve the consensus sequence of *NIP2;1*.

Plant material and Si quantification in grapevine leaves

Grape berries, canes, flowers and leaves of cv. Vinhão were collected from a commercial vineyard near Guimarães, Portugal (41°25'16.6N 8°14'38.4W) with permission from the owner of the field (Noronha *et al.*, 2016). Flowers were collected at the stage EL-23 (50% caps off) and leaves were collected at the same time as mature berries. Canes were collected after harvest in autumn. Roots were obtained after inducing rooting on cuttings collected from the same commercial field (Antólin *et al.*, 2010).

Cell suspensions of *V. vinifera* L. cv. Gamay Fréaux were maintained on modified Murashige and Skoog (MS) medium, supplemented with 2% (w/v) sucrose in 250 mL flasks on a rotary shaker at 100 rpm at 23 °C. Cells were subcultured every 10 days by transferring 10 mL aliquots into 40 mL of fresh medium. To study the effect of Si supplementation, culture media was supplemented with 1.5 mM of Na₂SiO₃ and growth proceeded by 10 days. The corresponding amount of Na⁺ was added in the form of NaCl to the control cells. After treatments, cells were immediately frozen in liquid nitrogen and stored at -80°C.

Si accumulation in grapevine leaves was studied in cv. Vinhão cuttings obtained as described previously (Antólin *et al.*, 2010). Plants were watered for one month with a commercial fertilizer (NPK 7:5:6) supplemented with 1.5 mM Na₂SiO₃ (six plants) or 3 mM NaCl (control, three plants). The pH of all the solutions was adjusted to 6.0. The two older leaves from each plant (biological replicate) were collected, oven dried at 60 °C for 3 days, ground to a fine powder and pelleted and Si was quantified using X-ray fluorescence spectrometry (Niton XL3t955 GOLDD+ XRF; Ouellette *et al.*, 2017).

RNA isolation from grapevine tissues

Approximately 200 mg of sample was used for total RNA extraction, following the method described by Reid *et al.*, (2006) combined with the GRS Total RNA kit-Plant (GRISP). cDNA was synthesized from 1 µg of total RNA using the Xpert cDNA Synthesis Master-mix Kit (GRISP).

Real-time PCR studies

Quantitative real-time PCRs were prepared with Xpert Fast SYBR Blue (GRISP). Experiments were carried out in biological triplicates using *VvGAPDH* as an internal

control. To verify the absence of unspecific and primer-dimer amplification, melting curves were performed after each run. Data were analyzed using gene expression tool in the CFX Manager Software 2.0 (Bio-Rad). The primers used to study the expression of *VvNIP2;1* and *VvGAPDH* are described in Table S1. Normalization of the average expression value of the reference gene was performed as described previously (Livak and Schmittgen, 2001).

***VvNIP2;1* cloning and construction of destination vectors**

VvNIP2;1 was cloned using Gateway® technology. Primers bearing the attB sequences (Table S1) for site-specific recombination with the entry plasmid *pDONR221* were used for PCR amplification. Subsequently, recombination of the target genes containing the attB sites with the entry plasmid was performed by the BP clonase enzyme. The target genes carried in the entry plasmid were then recombined by the LR clonase enzyme into the *pH7WGF2* for sub-cellular localization and *pVV214* for plate growth assays. All constructs were confirmed by sequencing.

Subcellular localization of *VvNIP2;1*

The *pH7WGF2-VvNIP2;1* construct was introduced into *Agrobacterium tumefaciens* (EHA105 strain) and transient transformation of tobacco (*Nicotiana tabacum*) leaf epidermal cells was performed according to Sparkes *et al.*, (2006). Tobacco plants were infiltrated with the bacterial cultures and leaf discs were examined under the confocal microscope after 3 days. The plasma membrane marker AtPIP2.1-mCherry was used (Nelson *et al.*, 2007).

Growth experiments with boric acid and sorbitol

To confirm the capacity of *VvNIP2;1* to transport boric acid the *S. cerevisiae* strain YSH1172 overexpressing *VvNIP2;1* was grown to log phase. Cultures were adjusted to different OD₆₀₀ nm (1.0 and 0.1) and spotted on solid YNB medium with 2% glucose (control) or supplemented with 20 mM H₃BO₃. To study the role of *VvNIP2;1* in osmotic stress response the yeast strain was cultivated on solid YNB medium with 2% glucose (control) or supplemented with 2 M sorbitol.

Functional characterization of VvNIP2;1 by stopped-flow fluorescence

To study water transport, VvNIP2;1 was cloned into pUG35 plasmid (Table S1). The yeast strain YSH1172 (MAT α leu2::hisG trp1::hisG his3::hisG ura3-52 aqy1::KanMX4 aqy2::HIS3; Leitão *et al.*, 2012), that is a deletion mutant for aquaporins, was transformed with pUG35-VvNIP2;1 and with pUG35 (control) constructs. Prior to permeability assays, cells in 1.4 M sorbitol, 50 mM K-citrate buffer pH 5.1, were preloaded with the non-fluorescent precursor 5-(and-6)-carboxyfluorescein diacetate (CFDA, 1 mM, 10 min at 30°C), which is intracellularly hydrolyzed yielding the impermeable fluorescent form (CF) as described (Soveral *et al.*, 2007). Stopped-flow experiments were performed on a Hi-Tech Scientific PQ/SF-53 apparatus (Hi-Tech Scientific, UK) with 2 ms dead time, temperature-controlled, interfaced with a microcomputer, at 23 °C. For activation energy assays temperature ranged from 10 to 34 °C. Five runs were usually analyzed in each experimental condition. In each run 0.1 mL of cell suspension was mixed with an equal amount of hyperosmotic solution (sorbitol or glycerol 2.1 M, 50 mM K-citrate buffer pH 5.1) to reach inwardly directed gradients of solute, inducing cell shrinkage or cell re-swelling respectively. Fluorescence was excited using a 470 nm interference filter and detected using a 530 nm cutoff filter. The time course of cell volume change was followed by fluorescence quenching of the entrapped fluorophore (CF). The recorded fluorescence signals were fitted to a single exponential, from which the rate constant (k) of cell shrinking or re-swelling was used to calculate the osmotic water permeability P_f or the glycerol permeability P_{gly} ($P_f = k(V_o/A)(1/V_w \cdot osm_{out})$ and $P_{gly} = k(V_o/A)$, where V_w is the molar volume of water, V_o/A is the initial cell volume to area ratio, and osm_{out} is the final medium osmolarity after the osmotic shock. The activation energy (E_a) of transport was evaluated from the slope of Arrhenius plots ($\ln P_f$ or $\ln P_{gly}$ vs. $1/T$) (Leitão *et al.*, 2012).

Clark electrode assays

The YSH1172 aqy-null yeast strain was transformed with pVV214-VvNIP2;1 and pVV214 (control) constructs and pre-cultured in YNB+SC solid medium. Liquid cultures were then grown overnight. Cells were then washed three times and resuspended in water to a final $OD_{600nm} = 0.5$. H_2O_2 was then added to the cell suspension to a final concentration of 50 μM and the O_2 formation was followed with a Clark electrode coupled to an YSI 5300 Biological Oxygen Monitor (Noronha *et al.*,

2016). The rate of O₂ release by the yeast strain overexpressing *VvNIP2;1* was compared with control cells and used as a measure of H₂O₂ uptake.

Arsenite (As), germanium (Ge) and silicon (Si) uptake in oocytes

For the synthesis of capped RNA, the ORF of *VvNIP2;1* was amplified by PCR with the primers shown in Table S1. The fragment containing the ORF was inserted into the *Xenopus* oocyte expression vector pXβG-ev1 (Preston *et al.*, 1992) or Pol1 (Garneau *et al.*, 2018). Capped RNA was synthesized from the linearized vector by *in vitro* transcription with the mMESSAGE mMACHINE High Yield Capped RNA Transcription Kit (ThermoFisher). Oocytes were isolated from *Xenopus laevis*. Procedures for deflocculating, culture conditions and selection were the same as described previously (Mitani *et al.*, 2008; Garneau *et al.*, 2018).

For As and Ge measurements, a volume of 50 nL (1 ng nL⁻¹) *in vitro* cRNA transcripts was injected into the selected oocytes. A 50 nL of RNase-free water as a negative control, 50 nL of rice *Lsi1* cRNA as a positive control were also injected. After 1 d incubation, transport activity assay was performed with 1.0 mM germanium (Ge), an analog of Si, or 0.1 mM arsenite as described previously (Mitani-Ueno *et al.*, 2014). The Ge and As concentrations in the digested solution were determined by inductively coupled plasma–mass spectrometer (7700X; Agilent Technologies).

For Si measurements, the oocyte assay was performed as described by Garneau *et al.*, (2018) with some minor changes. Oocytes at stage 5 or 6 were injected with 25 nL of 1 ng/nL cRNA or an equal volume of H₂O as negative control and incubated for one day at 18 °C in Barth's (MBS) medium. Then, 10 sets of 10 oocytes for each condition were exposed to MBS solution containing 1.7 mM Si for 30 min. After exposure, oocytes were rinsed in solution containing 0.32 M sucrose and 5.0 mM HEPES (pH 7.4). Si quantification was performed with a Zeeman atomic spectrometer AA240Z (Varian, Palo Alto, CA, USA) equipped with a GTA120 Zeeman graphite tube atomizer. Data from the spectrometer were analyzed using JMP 9.0.2 (SAS institute Inc.). Three replicates were used for this assay.

Statistical analysis

Results were statistically analysed by Student's t-test and by analysis of variance test (one-way) using Prism v. 5 (GraphPad Software, Inc.). Post-hoc multiple comparisons

were performed using Tukey's HSD test. For each condition, differences between mean values are identified with different letters or asterisks.

Results

Si quantification in grapevine leaves

To clarify whether grapevine accumulates Si, own-rooted cuttings of cv. Vinhão were irrigated with a fertilizer supplemented with 1.5 mM Na₂SiO₃ or 3 mM NaCl (control). Si was undetected in leaves from control plants but reached a concentration of 0.21 ± 0.04 % dw one month after Si supplementation. Leaf expansion and plant growth were similar in Si-treated and control plants (Fig. 1).

In silico analysis shows that VvNIP2;1 is a bona-fide silicon channel

As a first approach to evaluate if grapevine could express a putative Lsi, a phylogenetic analysis was performed with VvNIP2;1 and several aquaporins deemed permeable to Si (Fig. 2). Results showed that VvNIP2;1 clusters with other NIP proteins of Group III able to transport Si (Fig. 2). Moreover, protein sequence alignment of VvNIP2;1 with other Si transporters showed that these proteins share six transmembrane domains, two NPA motives separated by 108 aa and a GSGR Ar/R selectivity filter (Fig. 3; Deshmukh *et al.*, 2013).

VvNIP2;1 is a plasma membrane transporter mostly expressed in grapevine roots

The sub-cellular localization of VvNIP2;1 was studied following transient expression of a GFP-VvNIP2;1 in *Nicotiana tabacum* epidermal cells (Fig. 4). Results showed that VvNIP2;1 localizes to the plasma membrane, as indicated by the clear overlay with the plasma membrane marker AtPIP2.1 in leaves co-expressing AtPIP2.1-mcherry (Nelson *et al.*, 2007).

The expression pattern of *VvNIP2;1* in different grapevine tissues was assessed by qPCR (Fig. 5). Results showed that *VvNIP2;1* was highly expressed in roots but the steady-state transcript levels were also high in green berries and flowers.

VvNIP2;1 transports silicon and arsenic in *Xenopus* oocytes

To examine transport activity for silicon and arsenite, *VvNIP2;1* and *Lsi1* (as a positive control) cRNAs were injected into oocytes and uptake experiments were performed with As, germanium (an analog of Si) and Si. Results clearly showed that VvNIP2;1 is

able to mediate the transport of Ge and Si (25.88 ± 0.98 and 6.58 ± 0.90 ng oocyte⁻¹ 30 min⁻¹, respectively) and As (7.61 ± 0.42 ng oocyte⁻¹ 30 min⁻¹) at similar rates measured for the positive control Lsi. Basal transport was measured when oocytes were only injected with water (Fig. 6).

Overexpression of VvNIP2;1 in *Saccharomyces cerevisiae* supports boron and H₂O₂ transport but not water and glycerol

To evaluate the capacity of VvNIP2;1 to facilitate the transport of boron, the aqy-null mutant YSH1172 overexpressing VvNIP2;1 was cultivated in solid media supplemented with toxic concentration of this metalloid (Fig. 7A). Control growth experiments were performed with yeasts transformed with the empty vector. Results showed that the overexpression of VvNIP2;1 seemed to limit yeast growth in the presence of 20 mM boron.

Furthermore, the addition of 50 μM H₂O₂ to a suspension of transformed yeasts overexpressing VvNIP2;1 promoted an increased rate of O₂ release (produced after intracellular breakdown of H₂O₂) compared to the control, as measured with a Clark electrode (Fig. 7B).

Permeability experiments by stopped-flow fluorescence with transformed yeast cells showed VvNIP2;1 was unable to mediate water and glycerol transport (Table 1). Interestingly, transformed yeasts were more sensitive to a hyperosmotic medium (+ 2 M sorbitol; Fig. 7A).

Silicon supplementation does not affect the growth, anthocyanin and phenolic content, and VvNIP2;1 expression in grapevine cultured cells

It has been showed that Si supplementation increases plant's fitness under stress conditions, and an increase in the production of secondary compounds has also been described (Coskun *et al.*, 2019). Fig. 8 shows that when Gamay Freáux cultured cells (anthocyanin-accumulators) were cultivated for 12 days in liquid media supplemented with 1.5 mM Na₂SiO₃ growth was not affected nor the expression of VvNIP2;1. Also, no changes in anthocyanins and total phenolics were observed (Fig. 8).

Discussion

Up until now, Si transport in plants has been studied in a few species, mostly in cereal crops like rice and wheat, which are considered Si accumulators (Ma and Yamaji, 2006,

2015; Coskun *et al.*, 2019). Plant Si accumulation varies greatly among species and the capacity to accumulate Si in aerial parts has been attributed to the presence of transporters in the roots (Ma *et al.*, 2006; Chiba *et al.*, 2009; Coskun *et al.*, 2019). Interestingly, we found that grapevine, for which very little information exists about its Si accumulating capacity, expresses a NIP2 aquaporin that: i) clusters in group III, sharing all the features of a bona fide Si transporter (Fig. 2 and 3); ii) mediates the transport of Si, as confirmed by transport assays in oocytes (Fig. 6); iii) localizes at the plasma membrane (Fig. 4) and; iv) is expressed abundantly in roots (Fig. 5). Altogether, these features should allow grapevine to incorporate high amounts of Si from the soil. Incidentally, Si in the aerial parts of different field grown grapevines was shown to range from 0.44-0.73% dw and up to 2% in hydroponics, depending on the cultivar (Blaich and Grundhöfer, 1997), a value that would rank grapevine as a Si accumulator. Our results showed that own-rooted grapevine canes daily irrigated with 1.5 mM Si for one month accumulated only up to 0.25% dw in leaves, values well below 1%, which is usually indicative of a Si accumulator. In similar experiments with strawberry, Ouellette *et al.*, (2017) recorded the presence of functional Lsi1s in the species but showed that phenotypes of Si accumulation could be quite variable, from 0.1 to 3%, depending on the substrate and duration of the experiments. For instance, the authors showed that strawberry reached maximum accumulation of 3% after three months of fertilization, while values were only 0.2-0.3% after one month, similar to results obtained here. Additional experiments should look into longer periods of fertilization to determine the true potential of grapevine at accumulating Si. Future experiments should also be designed to evaluate if *VvLsi2*, which is present in grapevine genome (Fig. S1), is indeed a functional Si transporter, because it has been shown that this exporter cooperates with Lsi1 and is also fundamental for high Si accumulation (Ma *et al.*, 2007; Ma and Yamaji, 2015; Sun *et al.*, 2020).

Because most of Europe's grapevines are grafted, the capacity of the rootstock to incorporate Si could, at least theoretically, account for the plant capacity to accumulate Si in the aerial parts. The same happens with the role of the rootstock in the uptake of other nutrients, like calcium and magnesium (Gautier *et al.*, 2019). To address this issue, we analyzed the genome of four commercial rootstocks (1103P, M4, M1 and 101.14) and found that all share a *NIP2;1* gene with typical features of functional Si transporters (2 NPAs separated by 108 aa and a GSGR Ar/R filter; Fig. S2). Altogether, our results suggest that the presence of a *bona fide* Si transporter is a general feature of

Vitis sp. roots regardless of the capacity of the plants to accumulate Si in the aerial parts.

Besides Si, VvNIP2;1 was permeable to arsenite after expression in oocytes, similarly to rice Lsi1 and barley NIP2;1 (Bienert *et al.*, 2008; Ma *et al.*, 2008; Katsuhara *et al.*, 2014). Arsenite (As(3)) is abundant in anaerobic soils where typically rice is cultivated, but not in aerated soils where arsenate (As(5)) is the most abundant form. Thus, the observed arsenite transport capacity seems an ancestral feature shared by NIP2;1 with no, or very limited, biological significance in grapevine where As(5) is likely to be incorporated through phosphate transporters (Sun *et al.*, 2017).

Although previous studies have described water transport mediated by NIP aquaporins (Dean *et al.*, 1999; Wallace and Roberts 2005; Mitani-Ueno *et al.*, 2011; Katsuhara *et al.*, 2014), Garneau *et al.*, (2015) showed that Lsi1 had minimal transport activity compared to other AQPs. While VvNIP2;1 shares the same Ar/R filter with Lsi1 and HvNIP2;1, which are able to transport water (Mitani-Ueno *et al.*, 2011; Katsuhara *et al.*, 2014), yeast overexpressing VvNIP2;1 showed no water or glycerol transport activity (Table 1). Two functional Si transporters from different pumpkin cultivars were also unable to mediate water transport despite sharing the NPA and Ar/R filters of Lsi1 and HvNIP2;1 (Mitani *et al.*, 2011; Katsuhara *et al.*, 2014). Interestingly, although H₂O and H₂O₂ are structurally and electrostatically similar, VvNIP2;1 was able to distinguish both substrates, as previously observed for XIP aquaporins (Bienert *et al.*, 2011; Noronha *et al.*, 2016).

In this study, supplementation of grape cultured cells with 1.5 mM Na₂SiO₃ did not modify the production of anthocyanin and phenolics, nor the growth of the cells. Modifications in the secondary metabolism could be somewhat expected because the application of Si was shown to promote the accumulation of phenolics in rose (Shetty *et al.*, 2011) and other secondary metabolites (phytoalexins) in cucumber (Fawe *et al.*, 1998), rice (Rodrigues *et al.*, 2004) and wheat (Bélanger *et al.*, 2003; Rémus-Borel *et al.*, 2009). However, our results confirm several transcriptomic studies with rice, Arabidopsis, wheat and soybean that showed that Si had minimal effect on a plant's metabolism in absence of stress (Watanabe *et al.*, 2004; Fauteux *et al.*, 2006; Chain *et al.*, 2009; Rasoolizadeh *et al.*, 2018). In a recent review, Coskun *et al.*, (2019) suggested that Si had an indirect rather than a direct role on the multiple physiological/biochemical changes observed in stressed plants under Si treatment. Our experiments are, to our knowledge, among the first ones to assess directly on cultured

cells whether Si imparted biochemical but, while the expression of *NIP2;1* could be detected, the capacity of cultured cell to incorporate Si via a NIP2;1 protein still remains elusive. On the basis of our results, it does not appear that Si directly affects the secondary metabolism and that reports of such effects on plants are indeed attributable to other factors.

The protective effects of Si supplementation have been observed in several fruit species like cucumber, strawberry, banana and pepper against fungal attacks (Coskun *et al.*, 2019). In agreement, Si supplementation showed some level of protective role against powdery mildew in potted vines (Bowen *et al.*, 1992) and in field trials (Reynolds *et al.*, 1996). In this work, we present clear evidence regarding the identification, characterization and functionality of a Si transporter in grapevine roots, which suggests that adequate fertilization would allow grapevine to accumulate Si in the aerial part. In future work, the molecular mechanisms underlying the regulation of Si uptake at the root level, particularly with respect to VvLsi2-type transporters, the phenotypic variations associated with the fertilization regime, as well as the mechanisms behind its potential protective role in grape should provide useful information for Si supplementation in viticulture.

Acknowledgements

The work was supported by National Funds by FCT—Portuguese Foundation for Science and Technology, under the strategic programs UID/AGR/04033/2019 and UID/BIA/04050/2019. The work was also supported by FCT and European Funds (FEDER/POCI/COMPETE2020) through the research projects MitiVineDrought (PTDC/BIA-FBT/30341/2017 and POCI-01-0145-FEDER-030341) and BerryPlastid (PTDC/BIA-FBT/28165/2017 and POCI-01-0145-FEDER-028165). AS was supported by an FCT PhD grant (SFRH/BD/135782/2018). HN was supported by an FCT postdoctoral grant (SFRH/BPD/115518/2016).

References

- Antolín MC, Santesteban H, Ayari M, Aguirreolea J, Sánchez-Díaz. Grapevine fruiting cuttings, an experimental system to study grapevine physiology under water deficit conditions. In, *Methodologies and Results in Grapevine Research*, ed. Delrot S, Medrano H, Or E, Bavaresco L, Grando S. Springer 1ed 2010.
- Arkin AP, Cottingham RW, Henry CS, Harris NL, Stevens RL, Maslov S, *et al.*, 2018. KBase, The United States Department of Energy Systems Biology Knowledgebase. *Nature Biotechnology* 36, 566. doi, 10.1038/nbt.4163.
- Bélangier R, Benhamou N, Menzies J. 2003. Cytological evidence of an active role of silicon in wheat resistance to powdery mildew (*Blumeria graminis* f. sp. tritici). *Phytopathology* 93, 402-412.
- Bélangier R, Deshmukh R, Belzile F, Labbé C, Perumal A, Edwards SM. 2016. Plant with increased silicon uptake. Patent No, WO/2016/183684.
- Bienert GP, Bienert MD, Jahn TP, Boutry M, Chaumont F. 2011. Solanaceae XIPs are plasma membrane aquaporins that facilitate the transport of many uncharged substrates. *Plant Journal* 66, 306–317.
- Bienert GP, Thorsen M, Schüssler MD, Nilsson HR, Wagner A, Tamás MJ, Jahn TP. 2008. A subgroup of plant aquaporins facilitate the bi-directional diffusion of As(OH)₃ and Sb(OH)₃ across membranes. *BMC Biology* 6,26, doi,10.1186/1741-7007-6-26.
- Blaich R, Grundhöfer H. 1997. Uptake of silica by grapevines from soil and recirculating nutrient solutions. *Vitis* 36 (4), 161-166.
- Bowen P, Menzies J, Ehret D, Samuels L, Glass ADM. 1992. Soluble silicon sprays inhibit powdery mildew development on grape leaves. *Journal of the American Society for Horticultural Science* 117(6), 906-912.

Cabello-Hurtado F, Ramos J. 2004. Isolation and functional analysis of the glycerol permease activity of two new nodulin-like intrinsic proteins from salt stressed roots of the halophyte *Atriplex nummularia*. *Plant Science* 166, 633-640.

Chiba Y, Mitani N, Yamaji N, Ma JF. 2009. HvLsi1 is a silicon influx transporter in barley. *The Plant Journal* 57, 810-818.

Cochetel N, Escudí F, Cookson SJ, Dai Z, Vivin P, Bert PF, Muñoz MS, Delrot S, Klopp C, Ollat N, Lauvergeat V. 2017. Root transcriptomic responses of grafted grapevines to heterogeneous nitrogen availability depend on rootstock genotype. *Journal of Experimental Botany* 68(15), 4339-4355.

Corso M, Vannozzi A, Maza E, Vitulo N, Meggio F, Pitacco A, Telatin A, D'Angelo M, Feltrin E, Negri AS, Prinsi B, Valle G, Ramina A, Bouzayen M, Bonghi C, Lucchin M. 2015. Comprehensive transcript profiling of two grapevine rootstock genotypes contrasting in drought susceptibility links the phenylpropanoid pathway to enhanced tolerance. *Journal of Experimental Botany* 66(19), 5739-5752.

Coskun D, Deshmukh R, Sonah H, Menzies JG, Reynolds O, Ma JF, Kronzucker HJ, Bélanger RR. 2019. The controversies of silicon's role in plant biology. *New Phytologist* 221, 67-85.

Dean RM, Rivers RL, Zeidel ML, Roberts DM. 1999. Purification and functional reconstitution of soybean Nodulin 26. An aquaporin with water and glycerol transport properties. *Biochemistry* 38, 347-353.

Deshmukh RK, Vivancos J, Guérin V, Sonah H, Labbé C, Belzile F, Bélanger RR. 2013. Identification and functional characterization of silicon transporters in soybean using comparative genomics of major intrinsic proteins in *Arabidopsis* and rice. *Plant Molecular Biology* 83, 303-315

Deshmukh RK, Vivancos J, Ramakrishnan G, Guérin V, Carpentier G, Sonah H, Labbé C, Isenring P, Belzile FJ, Bélanger RR. 2015. A precise spacing between the NPA

domains of aquaporins is essential for silicon permeability in plants. *Plant Journal* 83, 489-500.

Fauteux F, Chain F, Belzile F, Menzies JG, Bélanger RR. 2006. The protective role of silicon in the Arabidopsis–powdery mildew pathosystem. *Proceedings of the National Academy of Sciences, USA* 103, 17554-17559.

Fawe A, Abou-Zaid M, Menzies J, Bélanger R. 1998. Silicon-mediated accumulation of flavonoid phytoalexins in cucumber. *Phytopathology* 88, 396-401.

Garneau AP, Carpentier GA, Marcoux AA, Frenette-Cotton R, Simard CF, Rémus-Borel W, Caron L, Jacob-Wagner M, Noël M, Powell JJ, Bélanger RR, Côté F, Isenring P. 2015. Aquaporins mediate silicon transport in humans. *PloS One*, 10(8), e0136149.

Garneau AP, Marcoux A, Frenette-Cotton R, Bélanger RR, Isenring P. 2018. A new gold standard approach to characterize the transport of Si across cell membranes in animals. *Journal of Cellular Physiology* 233, 6369-6376

Grégoire C, Rémus-Borel W, Vivancos J, Labbé C, Belzile F, Bélanger RR. 2012. Discovery of a multigene family of aquaporin silicon transporters in the primitive plant *Equisetum arvense*. *Plant Journal* 72, 320-330.

Hodson MJ, White PJ, Mead A, Broadley MR. 2005. Phylogenetic variation in the silicon composition of plants. *Annals of Botany* 96, 1027-1046.

Robinson JT, Thorvaldsdóttir H, Winckler W, Guttman M, Lander ES, Getz G, Mesirov JP. 2011. Integrative genomics viewer. *Nature biotechnology* 29, 24-26.

Katsuhara M, Sasano S, Horie T, Matsumoto T, Rhee J, Shibasaka M. 2014. Functional and molecular characteristics of rice and barley NIP aquaporins transporting water, hydrogen peroxide and arsenite. *Plant Biotechnology* 31, 213-219.

Kumar S, Stecher G and Tamura K. 2016. MEGA7, Molecular Evolutionary Genetics Analysis version 7.0 for bigger datasets. *Molecular Biology and Evolution* 33, 1870-1874.

Leitão L, Prista C, Moura TF, Loureiro-Dias MC, Soveral G. 2012. Grapevine aquaporins, gating of a tonoplast intrinsic protein (TIP2;1) by cytosolic pH, *PLoS One*. 7, e33219.

Livak KJ, Schmittgen TD. 2001. Analysis of relative gene expression data using real-time quantitative PCR and the $2^{-\Delta\Delta CT}$ method. *Methods* 25, 402-408.

Ma JF, Takahashi E. 2002. Soil, fertilizer, and plant silicon research in Japan. Amsterdam: Elsevier.

Ma JF. 2004. Role of silicon in enhancing the resistance of plants to biotic and abiotic stresses. *Soil Science and Plant Nutrition* 50, 11-18.

Ma JF, Tamai K, Yamaji N, Mitani N, Konishi S, Katsuhara M, Ishiguro M, Murata Y, Yano M. 2006. A silicon transporter in rice. *Nature* 440, 688-691.

Ma JF, Yamaji N, Mitani N, Tamai K, Konishi S, Fujiwara T, Katsuhara M, Yano M. 2007. An efflux transporter of silicon in rice. *Nature* 448, 209-212.

Ma JF, Yamaji N. 2015. A cooperative system of silicon transport in plants. *Trends in Plant Science* 20, 435-442.

Ma JF, Yamaji N, Mitani N, Xu XY, Su YH, McGrath SP, Zhao FJ. 2008. Transporters of arsenite in rice and their role in arsenic accumulation in rice grain. *Proceedings of the National Academy of Sciences* 105, 9931-9935.

Mitani N, Ma JF. 2005. Uptake system of silicon in different plant species. *Journal of Experimental Botany* 56, 1255-1261.

Mitani-Ueno N, Ogai H, Yamaji N, Ma JF. 2014. Physiological and molecular characterization of Si uptake in wild rice species. *Physiologia Plantarum* 151, 200-207.

Mitani N, Yamaji N, Ago Y, Iwasaki K, Ma JF. 2011. Isolation and functional characterization of an influx silicon transporter in two pumpkin cultivars contrasting in silicon accumulation. *The Plant Journal* 66, 231-240.

Mitani N, Yamaji N, Ma JF. 2009. Identification of maize silicon influx transporters. *Plant and Cell Physiology* 50, 5-12.

Mitani-Ueno N, Yamaji N, Zhao FJ, Ma JF. 2011. The aromatic/arginine selectivity filter of NIP aquaporins plays a critical role in substrate selectivity for silicon, boron, and arsenic. *Journal of Experimental Botany* 62, 4391-4398.

Montpetit J, Vivancos J, Mitani-Ueno N, Yamaji N, Remus-Borel W, Belzile F, Ma JF, Belanger RR. 2012. Cloning, functional characterization and heterologous expression of *TaLsi1*, a wheat silicon transporter gene. *Plant Molecular Biology* 79, 35-46.

Nelson BK, Cai X, Nebenführ A. 2007. A multicolored set of *in vivo* organelle markers for co-localization studies in Arabidopsis and other plants. *The Plant Journal* 51, 1126-1136.

Nicholas KB, Nicholas HB Jr, Deerfeld DW II. 1997. GeneDoc: analysis and visualization of genetic variation. *EMBNET.NEWS* 4, 14.

Noronha H, Araújo D, Conde C, Martins AP, Soveral G, Chaumont F, Delrot S, Gerós H. 2016. The grapevine Uncharacterized Intrinsic Protein 1 (VvXIP1) is regulated by drought stress and transports glycerol, hydrogen peroxide, heavy metals but not water. *PLoS ONE* doi: 10.1371/journal.pone.0160976.

Ouellette S, Goyette M., Labbé C, Laur J, Gaudreau L, Gosselin A, Dorais M, Deshmukh RK, Belanger RR. 2017. Silicon transporters and effects of silicon amendments in strawberry under high tunnel and field conditions. *Frontiers Plant Science* 8,949. doi,10.3389/fpls.2017.00949

Preston GM, Carroll TP, Guggino WB, Agre P. 1992. Appearance of water channels in *Xenopus* oocytes expressing red cell CHIP28 protein. *Science* 256, 385-387.

Rasoolizadeh A, Labbé C, Sonah H, Belzile F, Deshmukh RK, Menzies JG, Bélanger RR. 2018. Silicon protects soybean plants against *Phytophthora sojae* by interfering with effector-receptor expression. *BMC Plant Biology* 18,97.

Reid KE, Olsson N, Schlosser J, Peng F, Lund ST. 2006. An optimized grapevine RNA isolation procedure and statistical determination of reference genes for real-time RT-PCR during berry development. *BMC Plant Biology* 6,27.

Rémus-Borel W, Menzies JG, Bélanger RR. 2009. Aconitate and methyl aconitate are modulated by silicon in powdery mildew-infected wheat plants. *Journal of Plant Physiology* 166, 1413-1422.

Reynolds AG, Veto LJ, Sholberg PL, Wardle DA, Haag P. 1996. Use of potassium silicate for the control of powdery mildew [*Uncinula necator* (Schwein) Burrill] in *Vitis vinifera* L. cultivar Bacchus. *American Journal of Enology and Viticulture* 47(4), 421-428.

Rodrigues FA, McNally DJ, Datnoff LE, Jones JB, Labbé C, Benhamou N, Menzies JG, Bélanger RR. 2004. Silicon enhances the accumulation of diterpenoid phytoalexins in rice, a potential mechanism for blast resistance. *Phytopathology* 94, 177-183.

Rodrigues FA, Benhamou N, Datnoff LE, Jones JB, Bélanger RR. 2003. Ultrastructural and cytochemical aspects of silicon-mediated rice blast resistance. *Phytopathology* 93, 535-546.

Sabir F, Gomes S, Loureiro-Dias MC, Soveral G, Prista C. 2020. Molecular and functional characterization of grapevine NIPs through heterologous expression in aqy-null *Saccharomyces cerevisiae*. *International Journal of Molecular Sciences* doi,10.3390/ijms21020663

Shetty R, Fretté X, Jensen B, Shetty NP, Jensen JD, Jørgensen HJ, Newman MA, Christensen LP. 2011. Silicon-induced changes in antifungal phenolic acids, flavonoids, and key phenylpropanoid pathway genes during the interaction between miniature roses and the biotrophic pathogen *Podosphaera pannosa*. *Plant Physiology* 157(4), 2194-2205.

Soveral G, Madeira A, Loureiro-Dias MC, and Moura TF. 2007. Water transport in intact yeast cells as assessed by fluorescence self-quenching. *Applied and Environmental Microbiology* 73, 2341-2343.

Sparkes IA, Runions J, Kearns A, Hawes C. 2006. Rapid, transient expression of fluorescent fusion proteins in tobacco plants and generation of stably transformed plants. *Nature Protocols* 1, 2019-2025. PMID,17487191.

Sun H, Guo J, Duan Y, Zhang T, Huo H, Gong H. 2017. Isolation and functional characterization of CsLsi1, a silicon transporter gene in *Cucumis sativus*. *Physiologia Plantarum* 159(2), 201-214.

Sun H, Duan Y, Mitani-Ueno N, Che J, Jia J, Liu J, Guo, J, Ma J F, Gong H. 2020. Tomato roots have a functional silicon influx transporter, but not a functional silicon efflux transporter. *Plant, Cell & Environment* 43, 732-744.

Wallace IS, Roberts DM. 2005. Distinct transport selectivity of two structural subclasses of the nodulin-like Intrinsic Protein family of plant aquaglyceroporin channels. *Biochemistry* 44, 16826-16834.

Watanabe S, Shimoi E, Ohkama N, Hayashi H, Yoneyama T, Yazaki J, Fujii F, Shinbo K, Yamamoto K, Sakata K *et al.*, 2004. Identification of several rice genes regulated by Si nutrition. *Soil Science and Plant Nutrition* 50, 1273-1276.

Yamaji N, Chiba Y, Mitani-Ueno N, Ma JF. 2012. Functional characterization of a silicon transporter gene implicated in silicon distribution in barley. *Plant Physiology* 160, 1491-1497.

Zhao XQ, Mitani N, Yamaji N, Shen RF, Ma JF. 2010. Involvement of silicon influx transporter OsNIP2; 1 in selenite uptake in rice. *Plant Physiology* 153,1871-1877.

Accepted Manuscript

Table 1. Permeability coefficients and activation energies of water and glycerol transport of grapevine *VvNIP2;1* expressed in *Saccharomyces cerevisiae* following stopped-flow fluorescence. Yeast cells transformed with the *pUG35* vector were used as control.

		P_f (10^{-4} cm s $^{-1}$)	E_a (kcal mol $^{-1}$)
Water transport	<i>pUG35</i>	4.0 ± 0.28	14.05 ± 0.01
	<i>VvNIP2;1</i>	4.3 ± 0.27	13.55 ± 0.50
		P_{gly} (10^{-8} cm s $^{-1}$)	E_a (kcal mol $^{-1}$)
Glycerol transport	<i>pUG35</i>	1.55 ± 0.11	24.30 ± 1.20
	<i>VvNIP2;1</i>	1.45 ± 0.21	25.10 ± 0.80

Accepted Manuscript

Figure legends:

Figure 1. Si quantification in grapevine leaves from plants supplemented with 1.5 mM Na₂SiO₃ and 3 mM NaCl (control). Plants were watered with the corresponding solutions (pH 6.0) for one month and Si content analyzed by X-ray fluorescence spectrometry. N.D., not detected.

Figure 2. Phylogenetic analysis of several NIP proteins showing that they cluster into three distinct groups.

Figure 3. Protein alignment of several NIP2;1 proteins showing conserved NPA and Ar/R filters as well as the necessary 108 aa between the two NPAs.

Figure 4. Subcellular localization of VvNIP2;1 in *Nicotiana tabacum* mesophyll leaves following transient transformation by *Agrobacterium tumefaciens*. Co-localization studies were performed with the plasma membrane marker AtPIP2.1-mCherry.

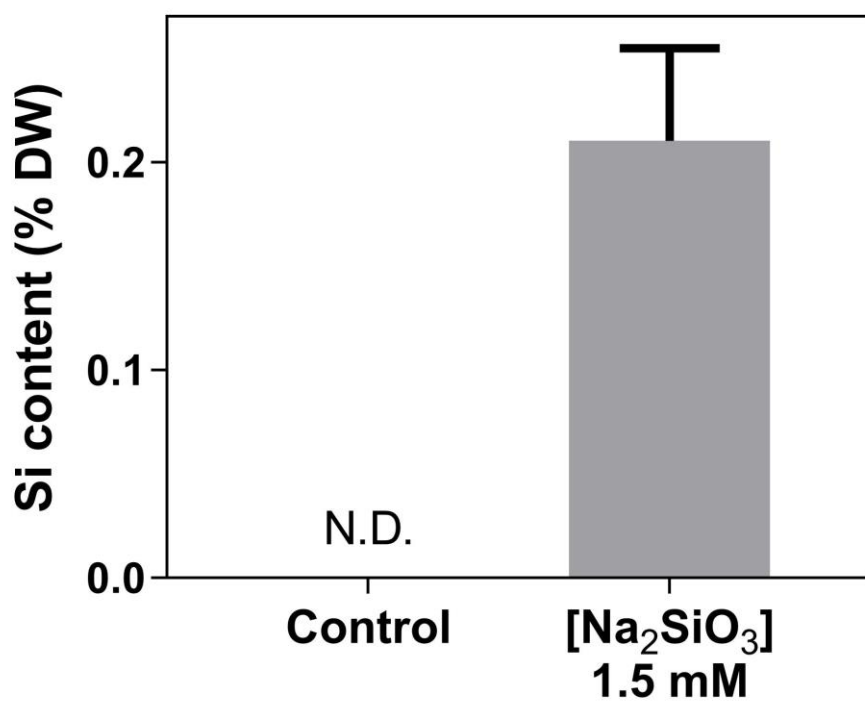
Figure 5. Expression of VvNIP2;1 by qPCR in different grapevine tissues. Values are mean ± SD and different letters indicate statistical significance ($P \leq 0.05$).

Figure 6. Transport of germanium (a), arsenic (b) and silicon (c) in oocytes injected with water and VvNIP2;1 and OsNIP2;1 (*Lsi1*) cRNAs (positive control). Values are mean ± SD and asterisks indicate statistical significance compared to the control (** $P \leq 0.0002$; **** $P \leq 0.0001$).

Figure 7. The effect of boric acid and sorbitol in the growth of *Saccharomyces cerevisiae* overexpressing VvNIP2;1 (A) and H₂O₂ transport measured in the O₂ electrode (B). *pVV214*, yeast transformed with empty vector (control); VvNIP2;1, yeast transformed with *pVV214-VvNIP2;1* plasmid. 0.1 and 0.01, yeast culture OD₆₀₀ nm.

Figure 8. Growth of cultured grape cells cv. Gamay Fréaux in media supplemented with 1.5 mM Si (a) and analysis of total phenolics (b), anthocyanins (c) and VvNIP2;1 expression (d) after 10 days of growth.

Figure 1



Accepted

Figure 2

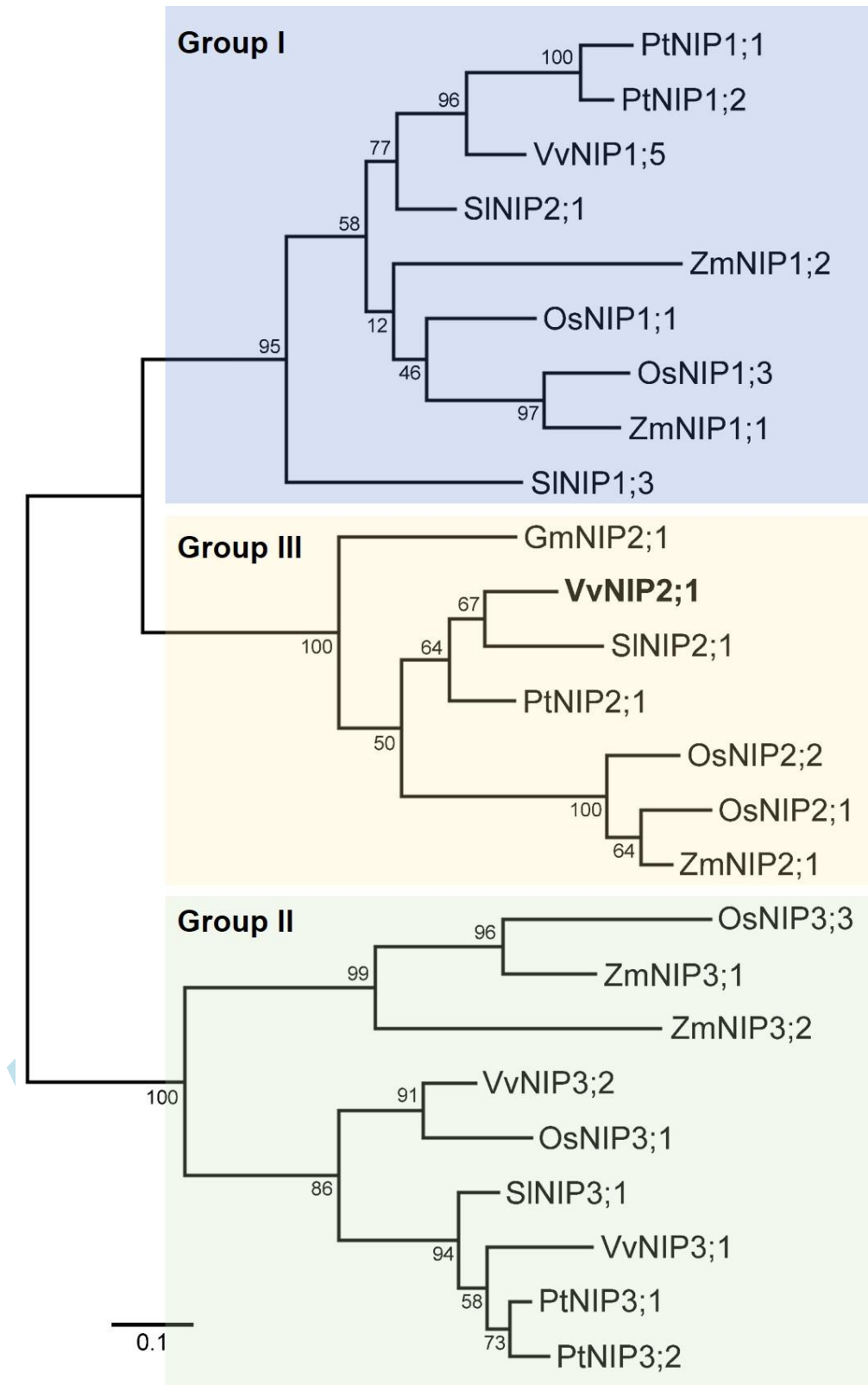
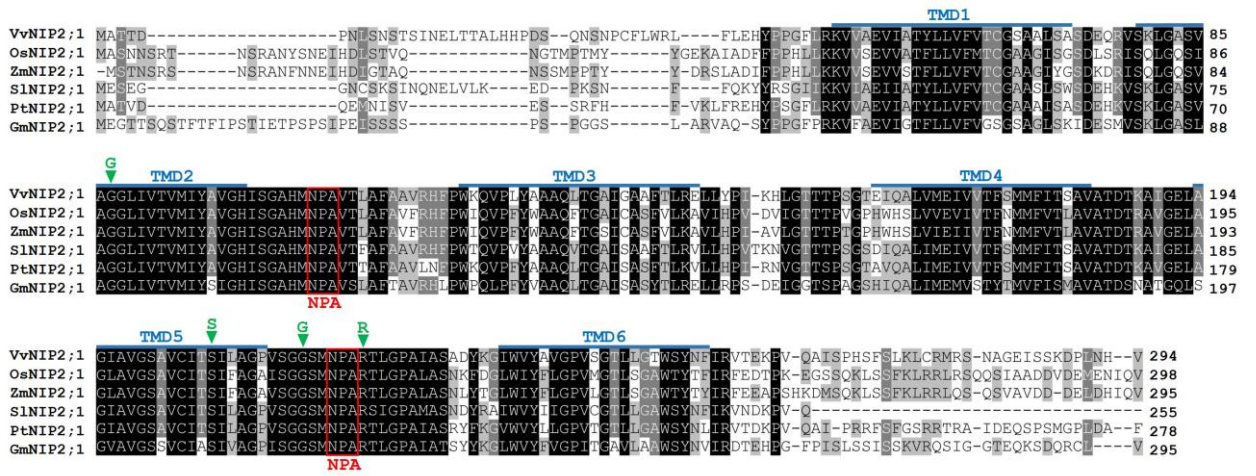
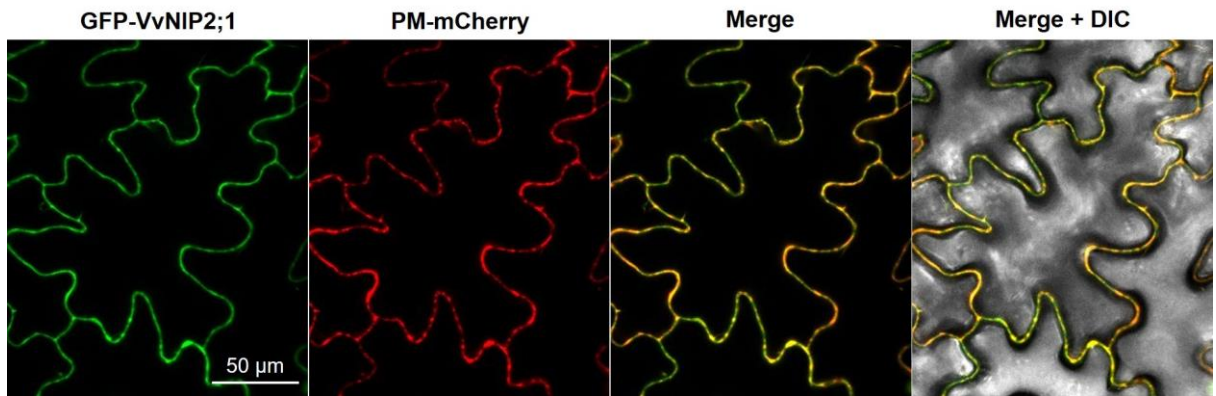


Figure 3



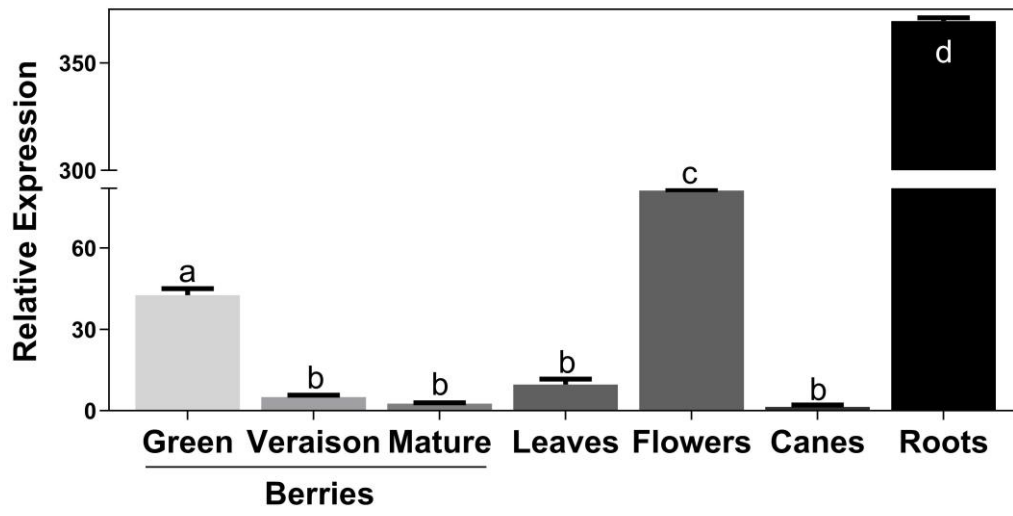
Accepted Manuscript

Figure 4



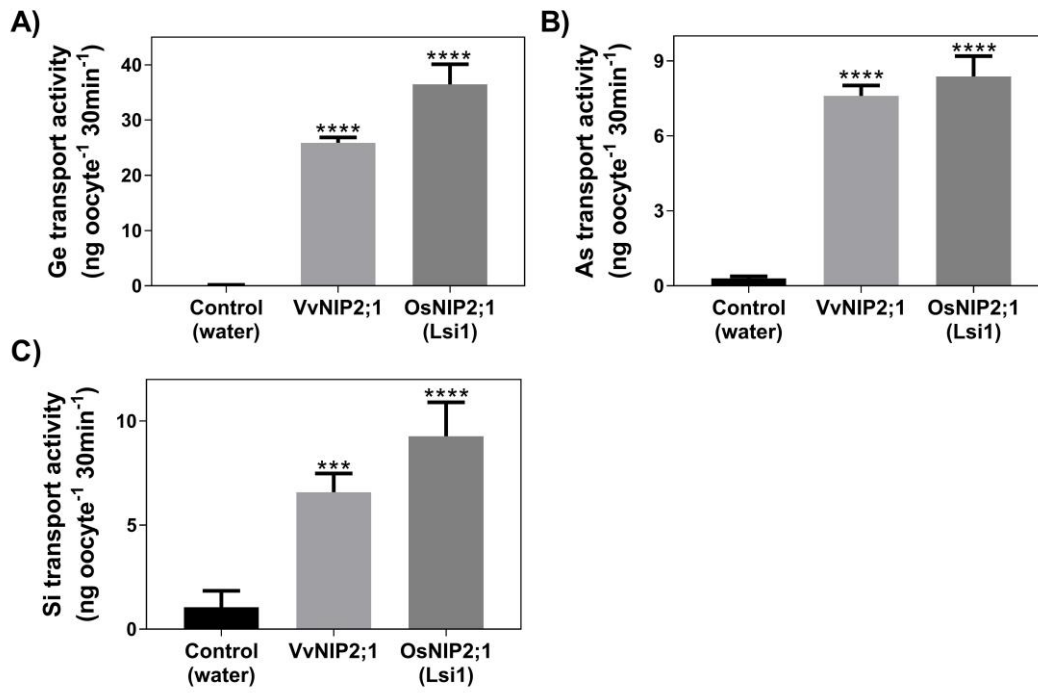
Accepted Manuscript

Figure 5



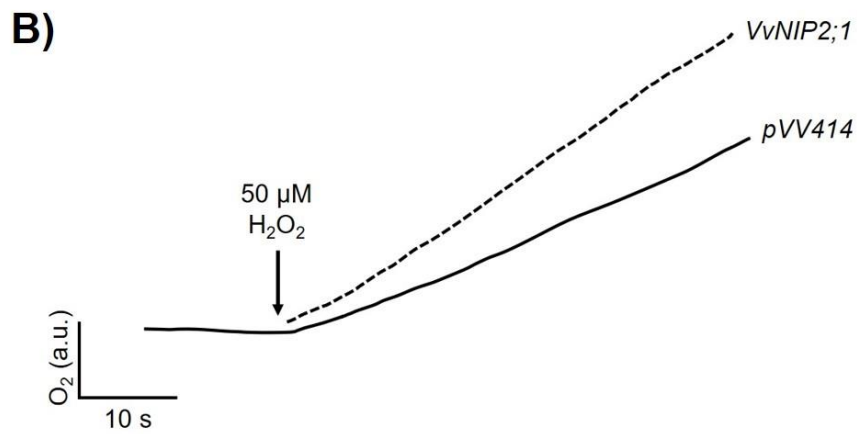
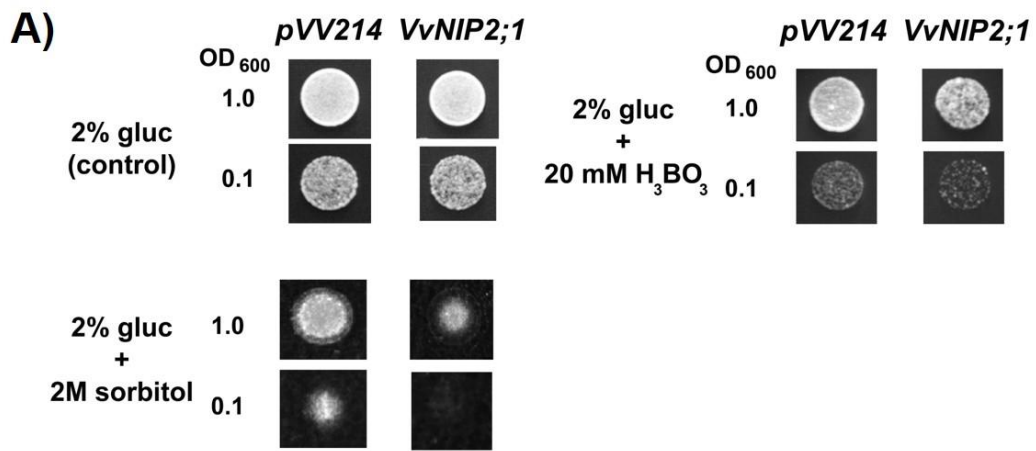
Accepted Manuscript

Figure 6



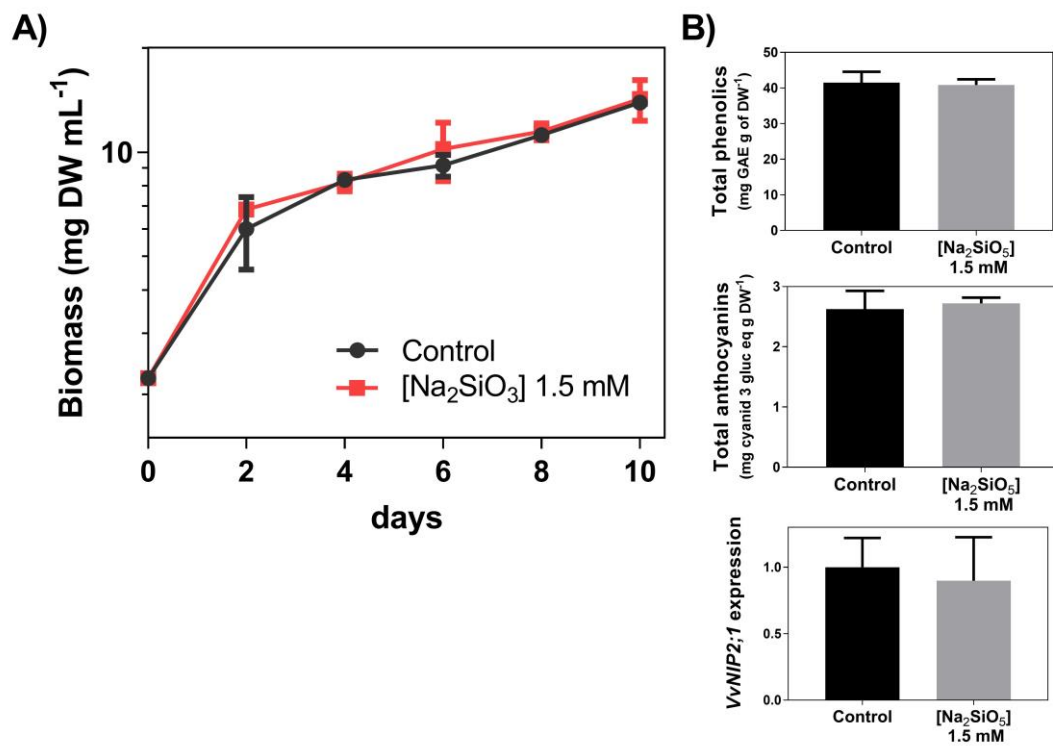
Accepted Manuscript

Figure 7



Accepted

Figure 8



Accepted